Computer Methods in Biomechanics and Biomedical Engineering
Vol. 7, No. 2, April 2004, pp. 79–89

Taylor & Francis
Taylor & Francis Group

A Multiscale Approach for Modelling Wave Propagation in an Arterial Segment

GIUSEPPE PONTRELLI*

Istituto per le Applicazioni del Calcolo-CNR Viale del Policlinico, 137-00161, Roma, Italy

(Received 29 August 2003)

A mathematical model of blood flow through an arterial vessel is presented and the wave propagation in it is studied numerically. Based on the assumption of long wavelength and small amplitude of the pressure waves, a quasi-one-dimensional (1D) differential model is adopted. It describes the non-linear fluid-wall interaction and includes wall deformation in both radial and axial directions. The 1D model is coupled with a six compartment lumped parameter model, which accounts for the global circulatory features and provides boundary conditions. The differential equations are first linearized to investigate the nature of the propagation phenomena. The full non-linear equations are then approximated with a numerical finite difference method on a staggered grid.

Some numerical simulations show the characteristics of the wave propagation. The dependence of the flow, of the wall deformation and of the wave velocity on the elasticity parameter has been highlighted. The importance of the axial deformation is evidenced by its variation in correspondence of the pressure peaks. The wave disturbances consequent to a local stiffening of the vessel and to a compliance jump due to prosthetic implantations are finally studied.

Keywords: Wall-fluid interaction; Wave propagation; Blood flow; Multiscale models; Numerical methods; Stent

INTRODUCTION

Mathematical models for cardiovascular system are largely used to simulate blood flow in arteries and to predict dynamical patterns in physiological and pathological conditions. Due to their complexity, comprehensive models are difficult to be settled. Such models depend on so many variables and parameters that, if not appropriately simplified, they raise more questions than useful answers. Complexity derives from geometry, time dependence and mechanical properties of the wall [1]. Any attempt to model all these aspects with an extreme degree of detail is to day destined to fail.

According to the specific scale of the phenomenon to be studied, various degrees of simplification at some levels have been proposed. One of them concerns the geometrical dimension of the model. In lumped parameters models, different complex regions of the vascular system are collected in simpler compartments and connected to form a closed loop, in analogy with the electrical circuits. The number of blocks is related with the degree of detail desired. Many lumped parameter models (also called 0D models) have been devised for the full cardiovascular system [2] and for specific vascular districts [3]. The main advantage of such an approach is the possibility to model the circulatory system and the blood pressure–velocity relationship with a relatively simple and computationally effective model. They provide the evolution of the mean flow variables but do not give any information on the mechanical fluid-wall interaction.

When wave propagation phenomena are of interest, one-dimensional (1D) models are commonly used. They constitute a higher degree of approximation and, based on the hypothesis that one spatial dimension is prevailing on the others, are obtained by averaging the motions equation over the cross section. Many features of the wave propagation in the arterial system can be understood on the basis of the linear theory. However, for an accurate representation and interpretation of observed waveforms, several non-linear effects are necessary to be included. The wave dynamics strictly depend on the interaction between blood flow and arterial wall. A collection of general problems on the fluid–structure interactions can

*Corresponding author. E-mail: g.pontrelli@iac.cnr.it

ISSN 1025-5842 print/ISSN 1476-8259 online © 2004 Taylor & Francis Ltd
DOI: 10.1080/1025584042000205868

be found in Ref. [4]. For applications in hemodynamics, an integral formulation for the fluid–wall system has been recently presented in Ref. [5].

Concerning the fluid forcing at the wall, many authors make the simplistic assumption that an instantaneous radial deformation of the wall takes place as a consequence of the transmural pressure. Actually, the tube deformation is related to the applied load by a set of differential equations expressing balances of forces between fluid and structure. Replacing them by an algebraic law corresponds in substituting dynamics of the tube by static, and leads to a gross approximation. A more realistic approach is obtained when the wall is modelled as a two-dimensional membrane that deforms under the forces exerted by the fluid [6]. Moreover, *in vivo* measurements evidence the presence of longitudinal stretch and stress [7]. Though much smaller than the radial displacement and generally neglected, the longitudinal wall motion needs a deeper study, since it revealed some importance in the analysis of the wall shear stress and may have interest in the investigation of pathologies. In this work, a simple 1D model for the fluid-structure problem describing the blood flow and the wave propagation in an arterial segment is presented. The wall constitutive equation for the vascular tissue proposed in Ref. [8] has been used in "The wall–fluid interaction" section. A linearization around a reference state is made to shed light on the nature of the phenomenon and the basic feature of the propagation features ("Analysis of the linearized system").

To take advantage of the 1D model and not give up to a simple description of the systemic circulation, the idea of coupling systems of different physical dimensions has been recently developed (multiscale approach) [9] and is re-proposed here. The matching interface conditions between a closed 0D model and a 1D model inserted at the level of descending aorta is addressed in "Coupling 0D and 1D models" section. Many computational results show the effectiveness of such heterogeneous approach and point out the dependence on the physical parameters ("Numerical results and discussion"). In "Effect of the stent insertion" section a case of clinical interest is finally studied.

THE WALL–FLUID INTERACTION

The blood flowing in a compliant vessel is a complex dynamical system and constitutes a genuine fluid–structure problem. The fluid motion and the wall deformation are mutually influenced and their coupling is responsible for effects which cannot be explained by each of them alone [4]. When wave propagation phenomena are concerned, simplified models for the system "blood-arterial wall" can be devised. In particular, due to the small deformations of the vascular wall and to the unidirectional nature of blood flow in an arterial segment, a 1D model is adopted.

The Flow Equations

Let us consider a homogeneous fluid of density ρ, viscosity μ, flowing in a straight, axisymmetric, distensible tube of circular cross section. A cylindrical coordinate system with x as the symmetry axis is used.

Let us consider the quasi-1D cross averaged momentum equation [1]:

$$\frac{\partial u}{\partial t} + u\frac{\partial u}{\partial x} = -\frac{1}{\rho}\frac{\partial p}{\partial x} + f \tag{2.1}$$

where u is the axial velocity, p the transmural pressure, both averaged over the cross section, and t denotes the time. The viscous term f is approximated by the friction term of the Poiseuille steady flow in a tube of radius R [9,10]:

$$f \simeq -\frac{8\mu u}{\rho R^2} \tag{2.2}$$

As a consequence, the wall shear stress is given by:

$$\tau = \mu\frac{\mathrm{d}u}{\mathrm{d}r}\bigg|_R \simeq \frac{4\mu u}{R} \tag{2.3}$$

Strictly speaking, the expressions (2.2) and (2.3) hold for a steady flow in a rigid tube, but they are considered acceptable for quasi steady flows and for small deformations. However, in 1D models for major arteries, the fluid viscosity and the wall shear stress can be neglected and the condition $\mu = 0$ is often encountered [1,10].

The principle of conservation of mass in a deformable tube is expressed by the following continuity equation [1]:

$$\frac{\partial R}{\partial t} + \frac{R}{2}\frac{\partial u}{\partial x} + u\frac{\partial R}{\partial x} = 0 \tag{2.4}$$

The Wall Equations

Due to its relatively small mass, compared with that of the fluid, the vessel wall is modelled as an elastic axisymmetric membrane, that is a 2D thin shell (wall thickness $\rightarrow$ 0). The membrane, which has no bending stiffness, is capable to deform under the forces exerted by the fluid (i.e. the shear stress τ and the transmural pressure p-cfr. Eq. (2.3)). Let $(x_P(s), r_P(s))$ be the Lagrangian coordinates of a particle P, with s a parametric coordinate along the membrane in its symmetry plane. In such reference frame, the principal deformation ratios in the axial and circumferential directions are respectively:

$$\lambda_1 = \sqrt{\left(\frac{\mathrm{d}r_P}{\mathrm{d}s}\right)^2 + \left(\frac{\mathrm{d}x_P}{\mathrm{d}s}\right)^2} \quad \lambda_2 = \frac{r_P}{R^*} \tag{2.5}$$

where R^* is the undeformed radius (corresponding to the zero transmural pressure).

Since the fluid equations are expressed in Eulerian coordinates, let us operate a transformation of coordinate and let us indicate by $R(x,t)$ and $S(x,t)$ the Eulerian counterparts of the Lagrangian coordinates of a particle of the membrane (see Ref. [6]). In such coordinate system, the stretches Eq. (2.5) are written as:

$$\lambda_1 = \sqrt{\frac{1+R'^2}{S'^2}} \qquad \lambda_2 = \frac{R}{R^*} \tag{2.6}$$

(the prime denotes x-derivative). By balance of forces, the fluid-membrane equilibrium equations in tangential and normal directions are provided [6]:

$$\begin{aligned} &R'(T_1 - T_2) + RT_1' = \tau R(1+R'^2)^{\frac{1}{2}} \\ &\frac{-R''}{(1+R'^2)^{\frac{3}{2}}}T_1 + \frac{1}{R(1+R'^2)^{\frac{1}{2}}}T_2 = p \end{aligned} \tag{2.7}$$

Let us now define a constitutive equation for the arterial vessel that give an expression for T_1 and T_2 in the Eq. (2.7). For an incompressible hyperelastic material, it is possible to define a strain-energy function W as a function of the principal strains: it represents the elastically stored energy per unit volume in terms of the strain variables and is a potential for the stress.

A constitutive strain-energy density function w modelling the mechanical properties of the arterial wall has been recently proposed by Zhou and Fung [8] as:

$$w = c_0(e^Q - 1) \quad Q = c_1E_1^2 + c_2E_2^2 + 2c_3E_1E_2 \tag{2.8}$$

where c_0 is a material parameter having the dimensions of dyn/cm, c_1, c_2, c_3 are non-dimensional constants (with $c_1 \approx c_2$ and $c_1, c_2 \gg c_3$) and $E_k = 1/2(\lambda_k^2 - 1)$ $k = 1, 2$ are the principal Green strains. Once the form of w is specified, the mechanical properties are completely determined, being the stress components (averaged across the thickness) along the longitudinal and circumferential directions given by differentiation of w:

$$\begin{aligned} T_1(\lambda_1,\lambda_2) &= \frac{\lambda_1}{\lambda_2}\frac{\partial w}{\partial E_1} = \frac{1}{\lambda_2}\frac{\partial w}{\partial \lambda_1} \\ &= 2\frac{\lambda_1}{\lambda_2}c_0e^Q(c_1E_1 + c_3E_2) \end{aligned} \tag{2.9}$$

$$\begin{aligned} T_2(\lambda_1,\lambda_2) &= \frac{\lambda_2}{\lambda_1}\frac{\partial w}{\partial E_2} = \frac{1}{\lambda_1}\frac{\partial w}{\partial \lambda_2} \\ &= 2\frac{\lambda_2}{\lambda_1}c_0e^Q(c_3E_1 + c_2E_2) \end{aligned} \tag{2.10}$$

The former relations hold in the case of an incompressible and anisotropic material, wherein principal directions of strain and stress coincide and express the property that the instantaneous Young's modulus increases with the strain, but with a different amount in the two directions [7]. Moreover, if $|\lambda_1| \approx 1$ (or in case of pure radial deformation), it follows $E_1 \approx 0$ and we approximate:

$$T_1 = \frac{1}{\lambda_2}c_0c_3e^Q(\lambda_2^2 - 1) \qquad T_2 = c_0c_2e^Q(\lambda_2^2 - 1)$$

In such a case, we have:

$$\frac{T_2}{T_1} = \frac{c_2}{c_3}\lambda_2^2$$

ANALYSIS OF THE LINEARIZED SYSTEM

Because of the complexity of the mathematical model, we proceed to a preliminary analysis by using a linearization of the variables in an infinite domain. This idealized case is justified because of the small wave amplitude and is useful to better understand the nature of the differential problem.

When a compliant tube filled with a liquid at rest or flowing with constant velocity is disturbed at one place, the disturbance will be propagated as a wave along the tube at finite speed. For simplicity, let us take a constant equilibrium unstressed state ($R^*, S^* = x, p^* \equiv 0, u^*$) as reference configuration,[†] and let us perturb the system with infinitesimal quantities ($\tilde{R}$, $\tilde{S}$, $\tilde{p}$, $\tilde{u}$):

$$R = R^* + \tilde{R} \quad S = x + \tilde{S} \quad p = 0 + \tilde{p} \quad u = u^* + \tilde{u} \tag{3.1}$$

In the hypothesis of waves of small amplitude and long wavelength, let us also assume that $\tilde{R}'$, $\tilde{R}''$, $\tilde{S}'$, $\tilde{u}_x$, $\tilde{p}_x$ and their time derivatives are infinitesimal of the same order.

By neglecting second and higher order infinitesimals, we have the following approximations (see Eq. (2.6)):

$$\sqrt{1+\tilde{R}'^2} \approx 1 + \frac{\tilde{R}'^2}{2} \approx 1 \quad \left(1 + \frac{\tilde{R}}{R^*}\right)^{-1} \approx 1 - \frac{\tilde{R}}{R^*}$$

$$\lambda_1 = \sqrt{\frac{1+\tilde{R}'^2}{(1+\tilde{S}')^2}} \approx \frac{1}{1+\tilde{S}'} \approx 1 - \tilde{S}' \tag{3.2}$$

$$\lambda_2 = \frac{R^* + \tilde{R}}{R^*} = 1 + \frac{\tilde{R}}{R^*}$$

It follows that:

$$E_1 = -\tilde{S}' \qquad E_2 = \frac{\tilde{R}}{R^*} \qquad Q = 0$$

Hence, by omitting second order terms:

$$\begin{aligned} T_1 &= 2c_0\left(-c_1\tilde{S}' + c_3\frac{\tilde{R}}{R^*}\right) \\ T_2 &= 2c_0\left(-c_3\tilde{S}' + c_2\frac{\tilde{R}}{R^*}\right) \end{aligned} \tag{3.3}$$

[†]For a viscous fluid, $u^* = 0$.

By replacing Eqs. (3.2) and (3.3) in Eqs. (2.1), (2.4) and (2.7) we obtain:

$$\tilde{R}' 2c_0\left[(c_3 - c_1)\tilde{S}' + (c_3 - c_2)\frac{\tilde{R}}{R^*}\right]$$
$$+ (R^* + \tilde{R})2c_0\left(-c_1\tilde{S}'' + c_3\frac{\tilde{R}'}{R^*}\right) = \pi(R^* + \tilde{R})$$
$$- \tilde{R}'' 2c_0\left(-c_1\tilde{S}' + c_3\frac{\tilde{R}}{R^*}\right)(R^* + \tilde{R})$$
$$+ 2c_0\left(-c_3\tilde{S}' + c_2\frac{\tilde{R}}{R^*}\right) = \tilde{p}R^*$$
$$\tilde{u}_t + (u^* + \tilde{u})\tilde{u}_x = -\frac{\tilde{p}_x}{\rho} + f(\tilde{u})$$
$$\tilde{R}_t + \frac{R^* + \tilde{R}}{2}\tilde{u}_x + (u^* + \tilde{u})\tilde{R}_x = 0$$

The first two terms in the first two equations are infinitesimal of second order and will be omitted. Thus, after integration (along x) of the first equation, the four equations reduce to:

$$2c_0\left(c_3\frac{\tilde{R}}{R^*} - c_1\tilde{S}'\right) = \int \tilde{\tau}\,\mathrm{d}x \equiv g(\tilde{u}) \tag{3.4}$$

$$2c_0\left(c_2\frac{\tilde{R}}{R^*} - c_3\tilde{S}'\right) = \tilde{p}R^* \tag{3.5}$$

$$\tilde{u}_t + u^*\tilde{u}_x = -\frac{\tilde{p}x}{\rho} + f(\tilde{u}) \tag{3.6}$$

$$\tilde{R}_t + \frac{R^*}{2}\tilde{u}_x + u^*\tilde{R}_x = 0 \tag{3.7}$$

The integration of the latter equations is accomplished in two steps: by first solving the wall configuration Eqs. (3.4) and (3.5) and then by updating the flow field Eqs. (3.6) and (3.7).

Wall Equilibrium Configuration

Let us suppose the flow variables $\tilde{p}$ and $g(\tilde{u})$ are known at a certain time. By solving Eqs. (3.4) and (3.5) with respect to $\tilde{R}$ and $\tilde{S}'$ we get:

$$\tilde{R} = \frac{R^*(c_3 g(\tilde{u}) - c_1\tilde{p}R^*)}{2c_0(c_3^2 - c_1c_2)} \quad \tilde{S}' = \frac{c_2 g(\tilde{u}) - c_3\tilde{p}R^*}{2c_0(c_3^2 - c_1c_2)} \tag{3.8}$$

The value of the perturbed deformations are inversely proportional to c_0 and do not depend on $\tilde{p}$ and $g(\tilde{u})$ only, but also on the reference value $R*$. For an inviscid fluid, we have $g(\tilde{u}) = 0$ and $\tilde{R}/R^* = (c_1/c_3)\tilde{S}'$.

Flow Field

Once the wall configuration is computed at a given time, the fluid dynamics variables are updated as follows. Let us now suppose that the viscous resistance is negligible ($f(\tilde{u}) = g(\tilde{u}) = 0$).

By replacing the expression Eq. (3.8) into Eqs. (3.6) and (3.7) we get the first order linear system:

$$\tilde{u}_t + u^*\tilde{u}_x + \frac{\tilde{p}_x}{\rho} = 0$$
$$\tilde{p}_t + \frac{c_0(c_1c_2 - c_3^2)}{c_1R^*}\tilde{u}_x + u^*\tilde{p}_x = 0$$

that is:

$$\mathbf{w}_t + \mathbf{A}\mathbf{w}_x = 0 \tag{3.9}$$

where

$$\mathbf{w} = \begin{pmatrix}\tilde{u}\\ \tilde{p}\end{pmatrix} \qquad \mathbf{A} = \begin{pmatrix} u^* & \frac{1}{\rho} \\ \frac{c_0(c_1c_2 - c_3^2)}{c_1R^*} & u^*\end{pmatrix}$$

The eigenvalues of $\mathbf{A}$:

$$\lambda_{1,2} = u^* \pm \sqrt{\frac{c_0(c_1c_2 - c_3^2)}{c_1\rho R^*}}$$

are real and distinct (system of hyperbolic type) and the characteristics are the straight lines:

$$\frac{\mathrm{d}x_1}{\mathrm{d}t} = \lambda_1 \qquad \frac{\mathrm{d}x_2}{\mathrm{d}t} = \lambda_2 \tag{3.10}$$

The system Eq. (3.9) can be put in normal form as follows. By defining:

$$\gamma = \sqrt{\frac{c_0(c_1c_2 - c_3^2)}{c_1\rho R^*}} > 0 \qquad \mathbf{G} = \begin{pmatrix}\gamma & 1\\ -\gamma & 1\end{pmatrix}$$
$$\mathbf{\Lambda} = \mathrm{diag}(\lambda_1, \lambda_2) = \begin{pmatrix} u^* + \gamma & 0 \\ 0 & u^* - \gamma\end{pmatrix} \tag{3.11}$$

we have:

$$\mathbf{G}\mathbf{A} = \mathbf{\Lambda}\mathbf{G} \tag{3.12}$$

Let $\mathbf{W} = \mathbf{G}\mathbf{w}$. Combining Eqs. (3.9) and (3.12) we obtain:

$$\mathbf{W}_t + \mathbf{\Lambda}\mathbf{W}_x = 0 \tag{3.13}$$

or, in scalar form:

$$(\tilde{p} + \gamma\tilde{u})_t + (u^* + \gamma)(\tilde{p} + \gamma\tilde{u})_x = 0$$
$$(\tilde{p} - \gamma\tilde{u})_t + (u^* - \gamma)(\tilde{p} - \gamma\tilde{u})_x = 0$$

Since in physiological regimes $u^* \ll \gamma$ the flow is subcritical and the characteristics have opposite sign. $W_1 = \tilde{p} + \gamma\tilde{u}$ and $W_2 = \tilde{p} - \gamma\tilde{u}$ are the two Riemann

invariants of the hyperbolic system Eq. (3.13): they do not vary along the characteristic lines Eq. (3.10) and concur to the formation of the pressure and flow pulses. The resulting solution is given by linear superposition of a progressive and of a regressive wave, with finite speeds $u^* + \gamma > 0$ and $u^* - \gamma < 0$, respectively.

The general solution of the system Eq. (3.13) in terms of $\tilde{p}$ and $\tilde{u}$ is given by:

$$\tilde{p} = \frac{W_1 + W_2}{2}$$

$$\tilde{u} = \frac{W_1 - W_2}{2\gamma}$$

A general analysis with similar arguments would be carried out when the linearization is around a reference (i.e. prestressed) state different from the unstressed configuration.

BOUNDARY CONDITIONS AND LUMPED PARAMETER MODELS

The linearized approach described in the previous section is not appropriate for the study of full non-linear system fluid–structure modelled by the coupled Eqs. (2.1), (2.4) and (2.7) and a numerical method will be used. The above differential equations have to be solved in a finite domain representing an arterial segment. Such a segment is extracted from the arterial tree and boundary conditions of physical significance for the variables are required. To this aim, the presence of the remaining vascular bed has to be considered. In Ref. [11], a pulsatile pressure is assigned at the inlet as a forcing, and a simple Windkessel 3-element parameter model for the termination is proposed. When balance of flows and pressures for the systemic circulation have to be taken into account, models for the closed-loop system should be addressed. They are built by partitioning the whole vascular tree in elementary districts and by "lumping" the dynamical variables in each of them (lumped parameter models). These models date back to the pioneeristic works of Westerhof *et al.*, and are based on the analogy between hydraulic networks and electrical circuits [12]. As example, in the network proposed by Avanzolini *et al.* [2] for the circulatory system, six sections can be recognized (see Fig. 1). In each compartment the values of the resistance, compliance and inertial parameters R_k, C_k, L_k are constant and a linear relationship between flow and pressure is given. These elementary blocks are linked between them and connected with the heart pump to form a closed loop representing the cardiovascular system. By setting conservation of pressure and flow rate in all nodes of the network, the following differential system is obtained:

$$\begin{aligned}
C_1 \frac{dx_1}{dt} &= \frac{s_1 z_1}{(R_l + R_1)} - x_2 \\
L_1 \frac{dx_2}{dt} &= x_1 - R_2 x_2 - x_3 \\
C_2 \frac{dx_3}{dt} &= x_2 - x_4 \\
L_2 \frac{dx_4}{dt} &= x_3 - R_3 x_4 - x_5 \\
C_3 \frac{dx_5}{dt} &= x_4 - \frac{s_2 z_2}{R_4} \\
\frac{dx_6}{dt} &= \frac{s_2 z_2}{R_4} - \frac{s_3 z_3}{(R_r + R_5)} \\
C_4 \frac{dx_7}{dt} &= \frac{s_3 z_3}{(R_r + R_5)} - x_8 \\
L_3 \frac{dx_8}{dt} &= x_7 - R_6 x_8 - x_9 \\
C_5 \frac{dx_9}{dt} &= x_8 - x_{10} \\
L_4 \frac{dx_{10}}{dt} &= x_9 - R_7 x_{10} - x_{11} \\
C_6 \frac{dx_{11}}{dt} &= x_{10} - \frac{s_4 z_4}{R_8} \\
\frac{dx_{12}}{dt} &= \frac{s_4 z_4}{R_8} - \frac{s_1 z_1}{(R_1 + R_l)}
\end{aligned} \tag{4.1}$$

The system describes the time evolution of the mean values of the variables in each compartment: x_i, $i = 1,3,5,7,9,11$ indicate pressure, while x_i, $i = 2,4,8,10$, refer to the flow rates. x_6 and x_{12} are the volume variation in right and in the left ventricle with respect to a reference volume. Finally, the variables s_i represent the state of two diodes simulating the cardiac valves and are such that:

$$s_i = \begin{cases} 1 & z_i > 0 \\ 0 & z_i \le 0 \end{cases} \tag{4.2}$$

depending on the sign of pressure gradient $z_i, i = 1, \ldots, 4$ at their ends. In Ref. [2] the authors simplify

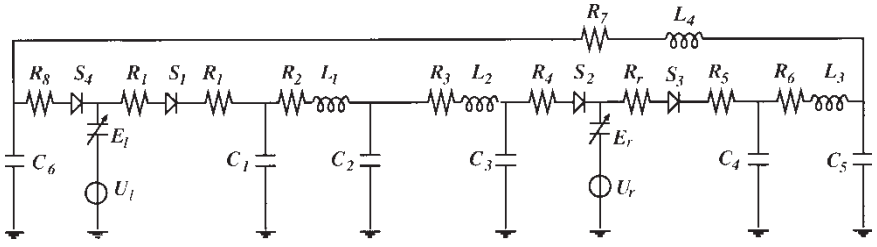

FIGURE 1 The electrical network analogue to a lumped parameter model at six compartments for the human circulatory system (see Avanzolini *et al.* [2]).

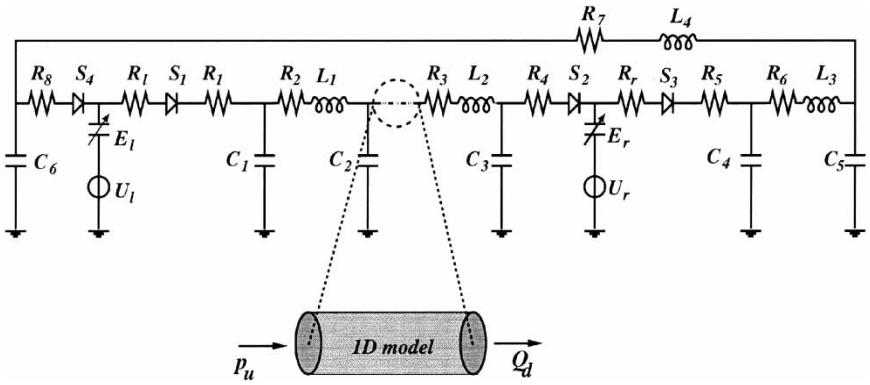

FIGURE 2 Coupling of 0D and 1D models at the level of the descending aorta. Pressure and flow variables are exchanged at the interface points to guarantee continuity (by courtesy of Formaggia *et al.* [9]).

the description of ventricular activity by linearizing the pressure–flow relation during the systolic phase. Moreover, the ventricular compliance during diastole is assumed constant. By indicating $\mathcal{V}_0$ a reference volume, we have:

$$P_v(t) = \begin{cases} U(t) + E(t)(\mathcal{V} - \mathcal{V}_0) + R\dot{\mathcal{V}} & \text{(Systole)} \\ E_d \cdot (\mathcal{V} - \mathcal{V}_0) & \text{(Diastole)} \end{cases} \tag{4.3}$$

where $\mathcal{V}$ is the ventricular volume and $\dot{\mathcal{V}}$ its time derivative. The isovolumic pressure and the ventricular elastance $E(t)$ are given by the following functions:

$$U(t) = U_0 a(t), \qquad E(t) = E_d + E_s\, a(t),$$

where

$$a(t) = \begin{cases} \frac{1}{2}\left[1 - \cos\left(\frac{2\pi t}{t_s}\right)\right] & 0 \le t < t_s \text{ (Systole)} \\ 0 & t_s \le t < t_c \text{ (Diastole)} \end{cases} \tag{4.4}$$

and t_s e t_c are the systolic and cardiac period, respectively.

The present 0D model represents a compromise between a quite high level of detail for the systemic circulation and computational simplicity and is used here as a prototype. The reader can refer to Ref. [2] for further details.

COUPLING 0D AND 1D MODELS

To account for a comprehensive system of the global circulation, the lumped model (a) described in "Boundary conditions and lumped parameter models" and the distributed model (b) presented in "The wall–fluid interaction" are coupled. This approach allows to implicitly assign boundary conditions for the system (b). Actually these are easily expressed as the functions of variables of (*a*) to guarantee the continuity of flow and pressure at the interfaces. Following Ref. [9], we have inserted the model (a) in the point of network corresponding to the descending aorta (Fig. 2). Consequently the 3rd and 4th Eqs. of system (4.1) has to be replaced by:

$$C_2 \frac{\mathrm{d}x_3}{\mathrm{d}t} = x_2 - Q_u \tag{5.1}$$

$$L_2 \frac{\mathrm{d}x_4}{\mathrm{d}t} = p_d - R_3 x_4 - x_5, \tag{5.2}$$

where Q_u and p_d indicate upstream flow rate and downstream pressure in model (b).

The coupled system (multiscale model) is equivalent to a 1D model for the full circulatory system where, except for a segment, the remaining arterial tree has been truncated and lumped in a finite number of blocks. On the other way around, the coupled model can be regarded as a lumped parameter model where a compartment has been expanded in a distributed model. The connected subsystems (a) + (b) form a unique closed-loop and no boundary condition for the flow variables is required.

If the coupling strategy eliminates the drawback of assigning a boundary value for u and p, wall displacement conditions at the extrema of the compliant vessel have to be provided. These are given by considering a long vessel[‡] with free ends. Therefore, the conditions:

$$R' = R'' = 0 \qquad S' = 1 \tag{5.3}$$

hold at the ends.[¶] From Eq. (2.7) it follows that the implicit relation for R:

$$Rp = T_2 \tag{5.4}$$

[‡]Here long means of length much larger than the reference radius $R*$.
[¶]The conditions (5.3) imply $\lambda_1 = 1$ (null axial strain), see Eq. (2.6).

(law of Laplace) unifies the three conditions (5.3) and is prescribed at the boundaries. Moreover, the boundary conditions on S:

$$S(0,t) = 0 \qquad S(L,t) = L^* \tag{5.5}$$

expressing a finite axial deformation are imposed.

Thus, we solve the differential system Eq. (4.1) (with the replacements of Eqs. (5.1) and (5.2)) and the partial differential system Eqs. (2.1), (2.4) and (2.7), together with interface continuity conditions. The algorithm proceeds as follows. At the first time step:

(1) The variables of the lumped system (a) are arbitrarily initialized. The values of Q_u and p_d are obtained as solution of the equilibrium configuration of system (b) with the boundary conditions $p_u = x_3(0)$ and $Q_d = x_4(0)$. In such a way the initial profile of the vessel segment is also computed.

From time t^k to time $(t + \Delta t)^{k+1}$, we proceed by solving alternately (a) and (b):

(2) The lumped system (a) is solved with the values Q_u^k and p_d^k in Eqs. (5.1) and (5.2).

(3) The distributed system (b) is updated. The interface conditions:

$$p_u^{k+1} = x_3^{k+1} \qquad Q_d^{k+1} = x_4^{k+1}$$

and the Eqs. (5.4) and (5.5) allow to solve the system (b) and to compute the new values Q_u^{k+1} and p_d^{k+1}. The profiles of R and S are also updated.

The procedure is repeated from point 2 at the following time steps [9,13].[§]

NUMERICAL RESULTS AND DISCUSSION

To solve the 1D fluid-structure model numerically, the Eqs. (2.1), (2.4) and (2.7) are solved simultaneously in a finite interval $[0,\mathcal{L}]$. Let us consider a sequence of $n+1$ equispaced grid points $(x_i)_{i=0,\ldots,n}$ with $x_0 = 0$ and $x_n = \mathcal{L}$. The spatial discretization is obtained by evaluating membrane strains and stresses (see Eqs. (2.6), (2.9) and (2.10)) at n inner points $\xi_i = (x_i + x_{i+1})/2$ of a staggered grid by considering averaged neighboring variables. On the other hand, wall–fluid equilibrium Eq. (2.7) and flow Eqs. (2.1) and (2.4) are computed at the $n-1$ inner points x_i [14]. In the following numerical experiments, the spatial mesh has been obtained by dividing the length of the vessel $L = 8\,\text{cm}$ in 800 equal parts ($\Delta x = 0.01\,\text{cm}$) and with a time step $\Delta t = 10^{-4}\,\text{s}$. The 1D model is inserted in correspondence of the descending aortic artery (Fig. 2) and is solved coupled with the 0D model. The Runge-Kutta scheme of second order has been used both in the distributed and the lumped parameter model to advance in time, as described in previous section. The choice of the above numerical values guarantees stability and grid independence. The resulting non-linear system is solved by a globally convergent Newton type method.

The following numerical values for the distributed model are used in Ref. [8]:

$$c_1 = 0.38 \quad c_2 = 0.26 \quad c_3 = 0.046$$

$$R^* = 0.8\,\text{cm} \quad L^* = L = 8\,\text{cm} \quad \rho = 1.05\,\text{g/cm}^3$$

In a large vessel, as that considered here, the frictional force due to the fluid viscosity is comparatively small and will be neglected. The condition $\mu = 0$ implies that $f = 0$ in Eq. (2.1) and $\tau = 0$ in Eq. (2.7) (see "flow equations"). The value of c_0 is varied in the range $c_0 = 10^5 - 10^7\,\text{dyn/cm}$ (note that c_0 in Eq. (2.8) is obtained by integration across the wall thickness of the analogous density energy function in Zhou and Fung [8]). For a lower value of c_0 the vessel wall undergoes large deformations that cannot be adequately represented by the present model. For $c_0 \gg 10^7$ the solution approaches to that relative of a rigid tube (see below). Actually, the values of R^*, p and c_0 cannot be chosen independently, but should satisfy a compatibility condition, being c_0 approximatively equal to pR (mean values), in the linear case. The same parameters R_k, C_k, L_k as in Ref. [2] for the lumped model have been used.[‖]

Subject to a positive heart pressure cycle Eq. (4.3), transmitted through the 0D model, the wall expands and oscillates periodically between a maximum and a minimum limits. Similarly, all the flow variables have a periodical behaviour. Actually we recognize a mean value and small-superposed fluctuations over it. Such values depend on the elasticity coefficient c_0 and of the undeformed radius R^*. In Fig. 3 the time history of the four variables u, p, R and S in the mid point are depicted for three different values of the parameter c_0. A small phase lead of p on u is present (see also Fig. 5). For larger c_0 the wall becomes stiffer: as expected, both the radial and longitudinal deformations decrease with c_0, being the latter comparatively smaller. Despite no significant variation in the pressure is present (a rise of the systolic peak of the pressure is obtained only at large c_0), a sharp increase of the flow velocity is reported, correspondent to the reduced arterial lumen. Some extra oscillations after the systolic peak may be present.

To measure the influence of c_0 on the radial deformation, let us introduce the mean deformation—referred to the central point ($x = 4$) and computed over the last two periods as:

$$\hat{R} = \frac{R_{\max} + R_{\min}}{2}$$

[§]Another possible strategy is to advance in time the 1D and 0D systems simultaneously.

[‖]Strictly speaking, such parameters would change when the 1D segment is inserted.

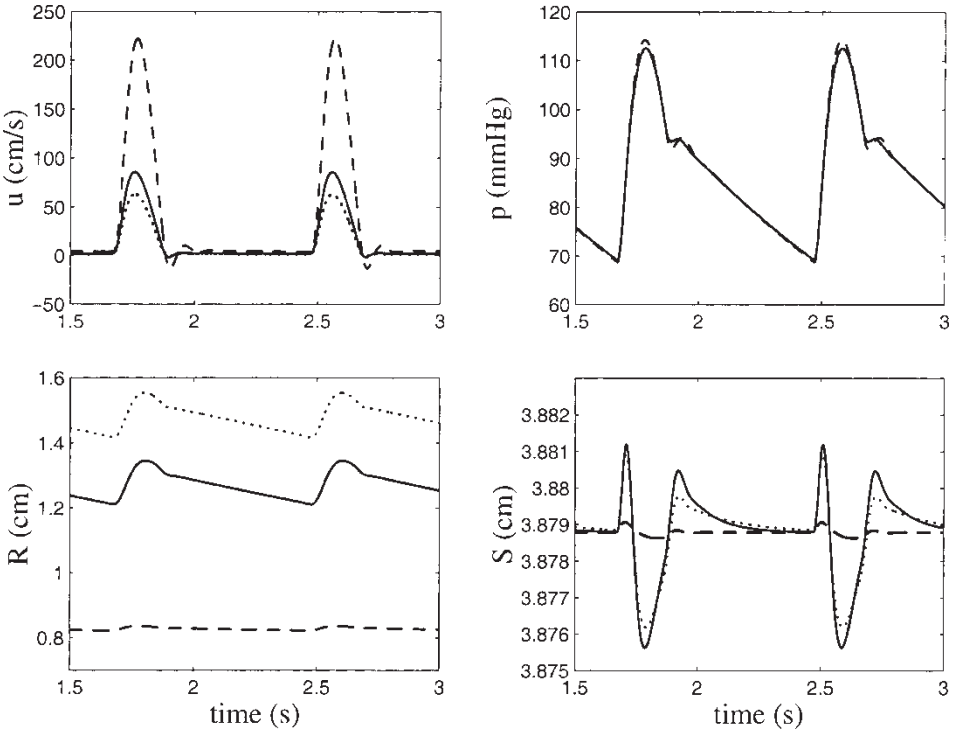

FIGURE 3 Time histories for u, p, R, S at the center of the artery for three values of the elasticity coefficient c_0($c_0 = 10^5$ dyn/cm dotted line, $c_0 = 2{\cdot}10^5$ dyn/cm continuous line, $c_0 = 5{\cdot}10^6$ dyn/cm dashed line).

the mean circumferential stretch $\hat{\lambda}_2 = \hat{R}/R^*$ and the non-dimensional radial amplitude $\hat{A} = (R_{\max} - \hat{R})/R^*$. Both $\hat{\lambda}_2$ and $\hat{A}$ drop (the former of 45%, the latter of 95%) with c_0 in the range considered, until an asymptotic value (Fig. 4).

The velocity of the wave can be obtained by fixing two points in the vessel and measuring the crossing time of a peak. However, such a procedure is not accurate over a short length and for the time and space steps as those selected in this work. Moreover, the profiles change their shape as they travel, and it is difficult to follow a profile in time. As a consequence, the computed speed value measured for u, p and R between the same grid points may be different, and varies in time. For $c_0 = 2{\cdot}10^5$ dyn/cm, an averaged value of the speed for u wave is found of about 6–7 m/s.

Khir and Parkers [15] suggest another method to measure the wave speed γ in elastic tubes in the absence of reflected waves. It is based on the validity of the water-hammer equation $\mathrm{d}p = \pm\rho\gamma\,\mathrm{d}u$ and consists in measuring the slope of the PU loop curves. For a typical PU loop as that displayed in Fig. 5, the local wave speed is $\gamma = 5.2$ m/s, in agreement with experiments. The theoretical estimate of γ in the linearized case (see Eq. (3.11)) predicts a much lower approximation of the wave speed (≈ 2.46 m/s). This is because an unstressed reference configuration has been considered.

EFFECT OF THE STENT INSERTION

One of the most frequent anomalies of the vascular system is the local stiffening of the wall due to the deposit of lipids and other substances. This induces the formation of an atherosclerotic plaque, which reduces the arterial lumen, and, to avoid surgical operations, the insertion of a endoprosthesis (stent) is a useful procedure to enlarge the arterial wall and to restore the correct flow. Despite its complex geometrical structure and a variety of mechanical characteristics, a stent can be schematically represented with a cylindrical meshed metal sleeve placed in the vessel to correct excessive narrowing of the section (i.e. stenosis) [16]. Although the stent implantation changes the geometry of the vessel and consequently induces important disturbances in the local flow, a relevant effect in the wall–fluid interaction are the change of the compliance due to the abrupt variation of the elasticity coefficient and the characteristics of the propagation [13].

In an artery of elasticity coefficient c_0, let us consider a stent of length 2σ centered in a point x^* and with elastic constant $c_s > c_0$. Therefore, the elasticity parameter along the stented artery is subjected to an abrupt change given by:

$$c(x) = \begin{cases} c_s & \text{if } |x - x^*| < \sigma \\ c_0 & \text{otherwise} \end{cases}$$

but, to avoid a compliance mismatch between the relatively rigid stented segment and the distensible vessel, the elastic

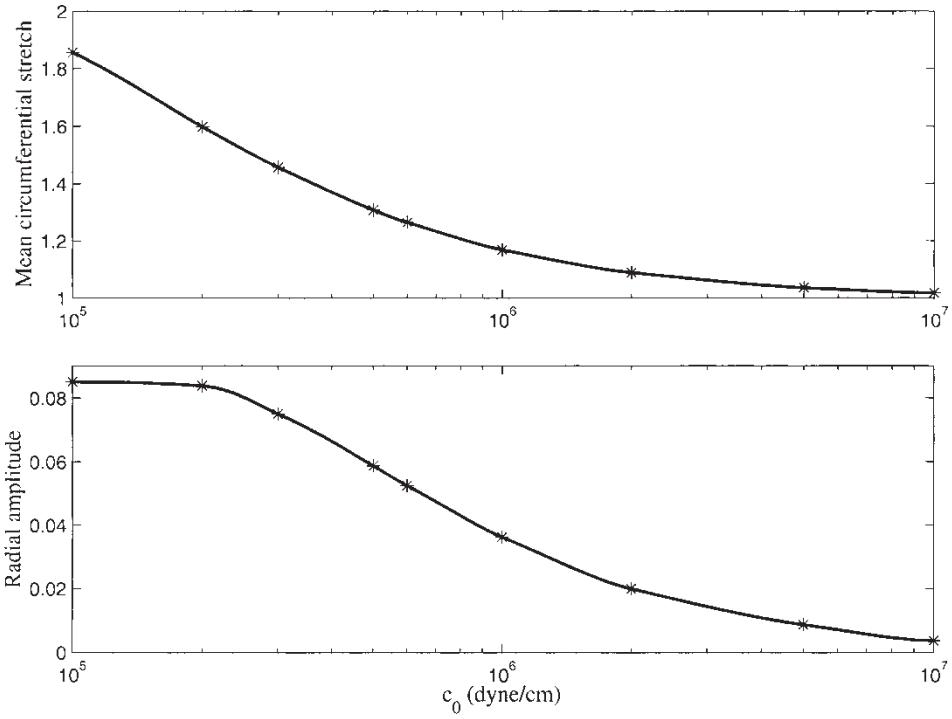

FIGURE 4 Mean circumferential stretch $\hat{\lambda}_2$ (above) and non-dimensional radial amplitude $\hat{A}$ (bottom) at the center of the vessel as a function of c_0. Starred points are results from simulations, continuous curves are obtained by a cubic interpolation. Note the different order of magnitude.

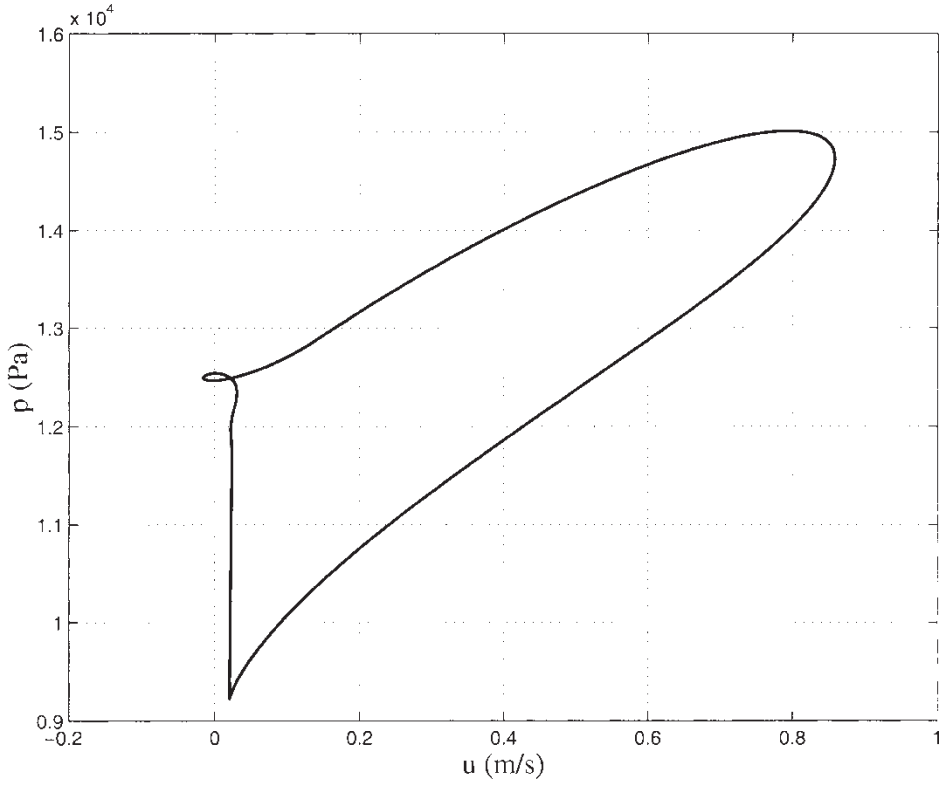

FIGURE 5 PU loop curve for $c_0 = 2{\cdot}10^5$ dyn/cm in the central point of the vessel. Slopes of such a curve indicates the local wave speed. A phase lag between the two variables is present.

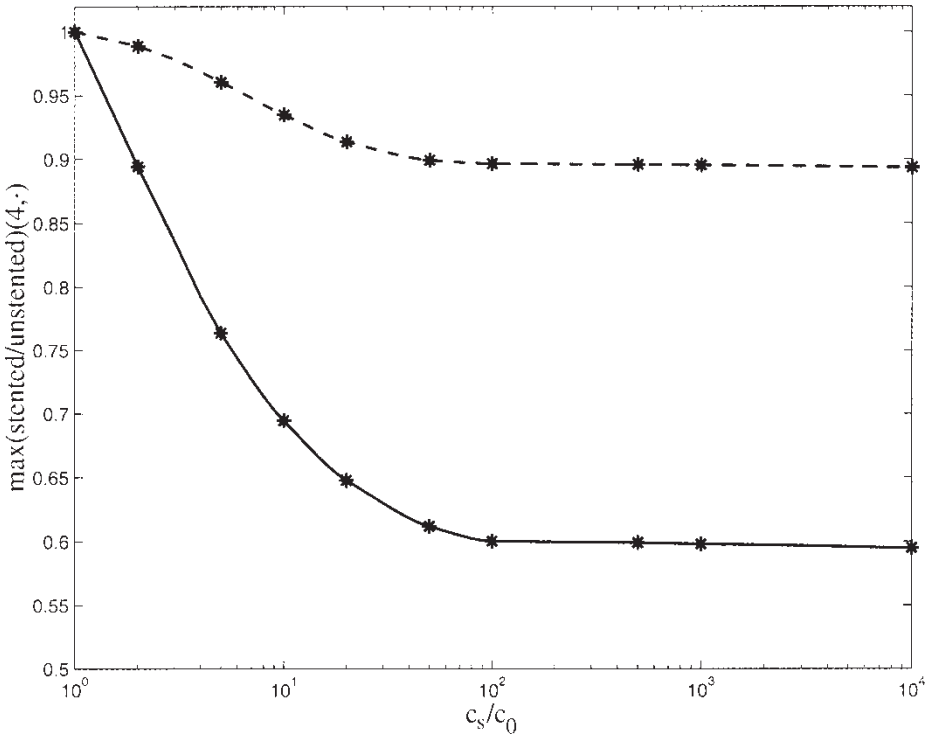

FIGURE 6 Ratio between the stented and unstented maximum values of the deformation (continuous line) and pressure (dashed line) at the center of the artery vs. $c_s/c_0 (c_0 = 2{\cdot}10^5\,\mathrm{dyn/cm},\ \sigma = 1\,\mathrm{cm})$. The values drop to the rigid tube values for $c_s \approx 100 c_0$.

parameter is modelled by a continuous rapidly changing function:

$$c(x) = c_0\left(1 + \delta \mathrm{e}^{-\left(\frac{x - x^*}{\sigma}\right)^8}\right) \qquad \delta = \frac{c_s - c_0}{c_0} \qquad (7.1)$$

(for $c_s = c_0$ an uniform elasticity coefficient is recovered). The effect of a physiological local hardening of an artery and the mechanical properties of stents can also be roughly modelled by varying the value of δ and σ.

In the numerical simulations, we fixed $\mathcal{L} = 8\,\mathrm{cm}$, $x^* = 4\,\mathrm{cm}$ $\sigma = 1\,\mathrm{cm}$, $c_0 = 2{\cdot}10^5\,\mathrm{dyn/cm}$ (corresponding to a stent 2 cm long placed at the center of the tube) and we varied c_s in Eq. (7.1) up to $c_s = 10^9\,\mathrm{dyn/cm}$.

As expected, the maximum values of the deformation and of the pressure at the center of the tube are reduced with c_s/c_0, and the asymptotic value of rigid wall is attained (Fig. 6). A sensible variation of the variables with respect of the unstented case occur only in correspondence of the peak of the systolic phase (Fig. 7), while the wave frequency remains unchanged with c. The crossing time of the wave in the stented artery is found up to three times lower than the correspondent time in the unstented case.

CONCLUSIONS

Mathematical models predicting the wave propagation characteristics of an arterial vessel are of interest for the clinicians. The outcome of such models constitute physiological indicators of diagnostic significance and

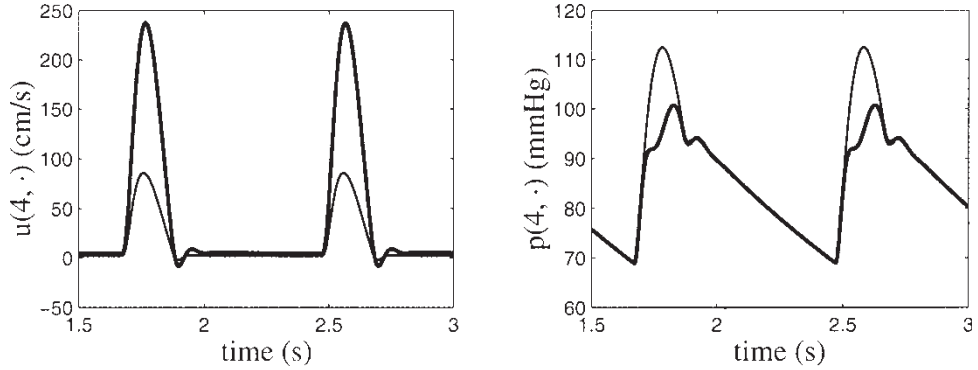

FIGURE 7 Time histories for u and p at the center of the stented artery (bold line), compared with the same variables in the unstented artery (thin line, cfr. Fig. 3) $(c_0 = 2{\cdot}10^5\mathrm{dyn/cm},\ c_s = 1000\,c_0,\ \sigma = 1\,\mathrm{cm})$.

their anomalies can be used to detect pathological states in vascular system.

The dynamics of the blood flow in an arterial segment has been studied in relation to the elastic non-linear properties of the vessel wall. The mechanical fluid–wall interaction is described by a 1D model and is expressed by a set of four non-linear partial differential equations. The hyperbolic nature of the propagation phenomenon has been analyzed in the linearized case. To account for a global circulation features, the distributed model has been coupled with a comprehensive lumped parameter model, which provide the proper boundary conditions by reproducing the correct waveforms entering into the vessel and avoid unphysical reflections at the outlet. This constitutes an improvement of the previous study where a simple Windkessel model has been used to approximate the arterial termination. For its multiscale structure, the present model depends on many physical, geometrical and material parameters. To discriminate among them, the emphasis has been put on the wall elasticity, which greatly affects the wave propagation. On the other hand, the fluid viscosity has been disregarded because of its small influence.

The model has some limitations: one is due to the mechanics of the wall, approximated as a thin shell with negligible inertia and no bending stiffness. Nevertheless, by including the longitudinal deformation, it reproduces the waveforms and the pressure pulse quite well, and offers a predictive insight in propagation phenomena. The model is adaptable for variable elastic properties of the vessel and the modified flow and structure pattern consequent to a prosthetic insertion has been investigated.

Numerical simulations have focused on the effect of the elastic properties on the flow and on the wall deformations and the results, though within a limited range of parameters, agree with physiological measurements with a good level of accuracy. The solution turns out to be much sensitive to the distributed and lumped parameters and a more realistic estimate of them should be done on the basis of experiments and clinical data.

References

[1] Fung, Y.C. (1997) Biomechanics: Circulation, 2nd Edn. (Springer-Verlag, New York).

[2] Avanzolini, G., Barbini, P., Cappello, A. and Cevenini, G. (1988) "CADCS simulation of the closed-loop cardiovascular system", *Int. J. Biomed. Comput.*, **22**, 39–49.

[3] Migliavacca, F., Pennati, G., Dubini, G., *et al.* (2001) "Modeling of the Norwood circulation: effects of shunt size, vascular resistance, and heart rate", *Am. J. Physiol. Heart Circ. Physiol.*, **280**, H2076–H2086.

[4] Païdoussis, M.P. (1998) Fluid–structure interactions—Slender structures and axial flow (Academic Press) Vol. **I**.

[5] Iemma, U. and Pontrelli, G. (2004) "An integral formulation for fluid-structure interaction in hemodynamics", In: Collins, M.W., Pontrelli, G. and Atherton, M.A., eds, Wall–fluid interactions in physiological flows (WIT Press), in press.

[6] Pedrizzetti, G. (1998) "Fluid flow in a tube with an elastic membrane insertion", *J. Fluid Mech.*, **375**, 39–64.

[7] Humphrey, J.D. (1995) "Mechanics of the arterial wall: review and directions", *Crit. Rev. Biomed. Eng.*, **23**(1/2), 1–162.

[8] Zhou, J. and Fung, Y.C. (1997) "The degree of non-linearity and anisotropy of blood vessel elasticity", *Proc. Natl Acad. Sci. USA*, **94**, 14255–14260.

[9] Formaggia, L., Nobile, F., Quarteroni, A. and Veneziani, A. (1999) "Multiscale modelling of the circulatory system: a preliminary analysis", *Comput. Visual Sci.*, **2**, 75–83.

[10] Porenta, G., Young, D.F. and Rogge, T.R. (1986) "A finite-element model of blood flow in arteries including taper, branches, and obstructions", *J. Biomech. Eng.*, **108**, 161–167.

[11] Pontrelli, G. and Rossoni, E. (2003) "Numerical modelling of the pressure wave propagation in the arterial flow", *Int. J. Numer. Meth. Fluids* **43**, 651–671.

[12] Westerhof, N., Bosman, F., Vries, C.D. and Noordergraaf, A.(1969) Analog studies of the human systemic arterial tree, *J. Biomech.*, Vol. **2**, 121–143.

[13] Formaggia, L., Nobile, F. and Quarteroni, A. (2001) A one dimensional model for blood flow: application to vascular prosthesis, MSCOM200, Lect. Notes Comp. Sci. Eng., (Springer-Verlag, Berlin).

[14] Fletcher, C.A. (1991) Computational techniques for fluid dynamics, *Springer Ser. Comp. Phys.*, Vol. **2**.

[15] Khir, A.W. and Parker, K.H. (2002) "Measurements of wave speed and reflected waves in elastic tubes and bifurcations", *J. Biomech.*, **35**, 775–783.

[16] Auricchio, F., Di Loreto, M. and Sacco, E. (2001) "Finite-element analysis of a stenotic artery revascularization through a stent insertion", *Comp. Meth. Biomech. Biochem. Eng.*, **4**, 249–263.